Expedited Articles

High-Resolution Crystal Structures of Human Cyclin-Dependent Kinase 2 with and without ATP: Bound Waters and Natural Ligand as Guides for Inhibitor Design†

Ursula Schulze-Gahmen, Hendrik L. De Bondt,‡ and Sung-Hou Kim*

Department of Chemistry and Lawrence Berkeley National Laboratory, University of California, Berkeley, California 94720, and Faculteit Farmaceutische Wetenschappen, Laboratorium voor Analytische Chemie en Medicinale Fysicochemie, K. U. Leuven, E. Van Evenstraat 4, B-3000 Leuven, Belgium

Received June 5, 1996⊗

Inhibition of the cell cycle is widely considered as a new approach toward treatment for diseases caused by unregulated cell proliferation, including cancer. Since cyclin-dependent kinases (CDKs) are key enzymes of cell cycle control, they are promissing targets for the design and discovery of drugs with antiproliferative activity. The detailed structural analysis of CDK2 can provide valuable information for the design of new ligands that can bind in the ATP binding pocket and inhibit CDK2 activity. For this objective, the crystal structures of human CDK2 apoenzyme and its ATP complex were refined to 1.8 and 1.9 Å, respectively. The high-resolution refinement reveals 12 ordered water molecules in the ATP binding pocket of the apoenzyme and five ordered waters in that of the ATP complex. Despite a large number of hydrogen bonds between ATP-phosphates and CDK2, binding studies of cyclic AMP-dependent protein kinase with ATP analogues show that the triphosphate moiety contributes little and the adenine ring is most important for binding affinity. Our analysis of CDK2 structural data, hydration of residues in the binding pocket of the apoenzyme, flexibility of the ligand, and structural differences between the apoenzyme and CDK2-ATP complex provide an explanation for the results of earlier binding studies with ATP analogues and a basis for future inhibitor design.

Introduction

Protein kinases are a large family of enzymes that are essential for the regulation of many diverse cell functions through phosphorylation of other enzymes and structural proteins.[1] Biochemical and structural studies have increased our understanding of their role in signal transduction[2−5] and cell cycle regulation[6−8] enormously in recent years. For example, crystal structures of several serine/threonine protein kinases, including cyclic-AMP-dependent protein kinase (cAPK),[9] mitogen-activated protein kinase (MAPK),[10] twitchin kinase,[11] casein kinase 1 (CK1),[12] phosphorylase kinase (PhK),[13] and cyclin-dependent kinase 2 (CDK2),[14] revealed a common two-domain core structure with enzyme-specific variations.[15]

Among protein kinases, CDK2 plays a central role in cell cycle regulation, and efforts are underway to develop specific inhibitors of CDKs as potential antimitogenic drugs.[16−19] Structure-based drug design requires the three-dimensional structure of the target enzyme and possibly its bound natural ligand or lead inhibitor compound. Hence, high-resolution data provide important information for the design of active ligands because more accurate protein structures including bound water molecules can be obtained. Hydration of residues that participate in protein−ligand interactions is important in determining the thermodynamics of ligand binding and provides clues for identifying protein residues as potential ligand interaction sites.

Previously reported crystal structures of the CDK2 apoenzyme and its ATP complex were refined to 2.4 Å,[14] where the details of hydration in the ATP binding pocket were not certain. We have now obtained high-resolution crystals and refined the structures of the apoenzyme to 1.8 Å and that of the ATP complex to 1.9 Å. Here, we describe in detail the interactions between ATP and CDK2, the coordination of the Mg^{2+} ion, and the ordered water structure in the binding pocket of the apoenzyme and discuss the implications of the structural information for the affinity of ligand binding.

Results and Discussion

Refinement. The details of data collection and reduction are summarized in Table 1. Refinement of the CDK2 apoenzyme and ATP complex to 1.8 and 1.9 Å, respectively, resulted in very accurate protein models as indicated by low *R* values, good stereochemistry (Table 2), and estimated coordinate errors of 0.2 Å for the apoenzyme and 0.2−0.25 Å for the ATP complex.[20] In the apoenzyme structure, all residue conformations fall in energetically favorable regions of the Ramachandran plot, and in the ATP−enzyme complex, only residue Val[44] adopts a conformation just outside the favorable conformations.[21] The electron density for both molecules is well defined with the exception of residues 37−40, which were omitted in both molecules. In addition, residues at the N-terminus and C-terminus

† The refined coordinates of CDK2 apoenzyme and CDK2-ATP complex have been deposited in the Protein Data Bank, Biology Department, Brookhaven National Laboratories, Upton, NY 11973, under the file names 1HCL and 1HCK, respectively.

‡ K. U. Leuven.

⊗ Abstract published in *Advance ACS Abstracts,* October 1, 1996.

S0022-2623(96)00402-5 CCC: $12.00

Table 1. Data Collection Statistics

	CDK2 apoenzyme	CDK2-ATP complex
space group	$P2_12_12_1$	$P2_12_12_1$
unit cell (Å)	$a = 73.12$, $b = 72.72$, $c = 54.25$	$a = 72.82$, $b = 72.66$, $c = 54.07$
resolution (Å)	$\infty - 1.8$	$\infty - 1.9$
unique reflections	27034 (3904)[a]	22636 (3019)[b]
multiplicity	3.6	3.6
completeness (%)	98.6 (97.1)[a]	97.3 (92.8)[b]
R_{merge} (%)[c]	6.12	6.75
I/σ_I	12 (2.4)[a]	10 (1.5)[b]

[a] Number in brackets is the corresponding value for resolution shell 1.9 to 1.8 Å. [b] Numbers in brackets are the corresponding values for resolution shell 2.0 to 1.9 Å. [c] $R_{merge} = \sum|I(h) - <I(h)>|/\sum I(h)$, where $I(h)$ is the observed intensity and $<I(h)>$ the mean intensity of reflection h over all measurements of $I(h)$ with $I/\sigma_I > 0$.

Table 2. Refinement Statistics

	CDK2−apoenzyme	CDK2−ATP complex
resolution (Å)	8−1.8	8−1.9
reflections ($F/\sigma_F > 2.0$)	22436	19547
atom		
protein	2373	2371
solvent	180	108
ATP		31
Mg		1
R_{free}[a]	25.45%	27.19%
R_{cryst}[a]	18.12	18.47
rms deviation[b]		
bonds (Å)	0.011	0.012
angles (deg)	1.61	1.78
dihedrals (deg)	24.18	24.58
improper (deg)	1.42	1.58
average B values (Å^2)		
CDK2	31	37
solvent	44	48

[a] $R_{value} = (\sum_{hkl}|F_o - F_c|)/\sum_{hkl}F_{obs}$, where R_{free} is calculated for a randomly chosen 10% of reflections omitted from refinement and R_{cryst} is calculated for the remaining 90% of reflections included in the refinement. [b] Root-mean-square deviations from ideal values.

and residues 72−75 and 153−162 have higher than average B values.

ATP Binding. The electron density for the refined CDK2−ATP complex shows clear density for the ATP molecule with all three phosphates, a Mg^{2+} ion, and five water molecules within 4.5 Å of the ATP molecule (Figure 1). The five-membered ribose ring is puckered into a C2′-*endo* envelop. The increased resolution allowed the identification of alternate side-chain conformations for Gln^{131}, which provide additional contacts with the β-phosphate (Figures 2 and 6). In the stronger occupied side chain conformation, the side-chain turns toward the backbone and the side-chain amide oxygen is within hydrogen bonding distance to the residue's own peptide nitrogen. In addition, it forms several van der Waals contacts with Pro^{130}. In the second, weaker occupied conformation, the side chain points into the binding pocket, forming a hydrogen bond with a β-phosphate oxygen of ATP. A total of 93 interatomic contacts between CDK2 plus bound waters and ATP were identified; 26 contacts with the adenine base, 15 with the ribose, and 52 with the phosphates (Table 3).

As can be expected from the relative hydrophilicity of the ATP molecule, most hydrogen bonds and salt bridges (9) are formed with the phosphate moiety, while the adenine base and ribose are involved in only three hydrogen bonds each (Figure 2, Table 3). Three water molecules, Wat^{502}, Wat^{503}, and Wat^{505}, in the binding pocket are also mediating CDK2−ATP interactions (Figure 2, Table 3).

The hexacoordinate Mg^{2+} ion is bound by one oxygen from each phosphate, and one each from Asn^{132} and Asp^{145} side chains and Wat^{503} (Figure 3) with coordination bonds ranging in length from 1.82 to 2.29 Å. The coordination of all three phosphates of ATP by a single Mg^{2+} ion is very unusual and to our knowledge has never been observed before. The electron density for the Mg^{2+} ion is relatively weak which is reflected in the refinement of its occupancy to 0.6 with a B value of 32 Å^2.

ATP Binding Pocket in the Apoenzyme and Comparison with CDK2−ATP Complex. The excellent electron density for the apoenzyme structure allowed the placement and refinement of 180 water molecules in hydrogen bonding distance to the protein. Water molecules in the ATP binding pocket area are especially interesting with regard to analyzing ligand binding and designing new ligands. We identified 12 water molecules that are overlapping with or are within 4.2 Å of the ATP ligand after superposition of the apoenzyme and the enzyme−ATP complex (Figure 4). Three water positions of the apoenzyme are retained in the CDK2−ATP complex (Figure 5), but only one of these, Wat^{503}, is within van der Waals distance to ATP and forms hydrogen bonds with the Mg^{2+} ion and the ribose O5′ (Table 3). Waters in the other two common positions are hydrogen bonded to Asp^{145} peptide nitro-

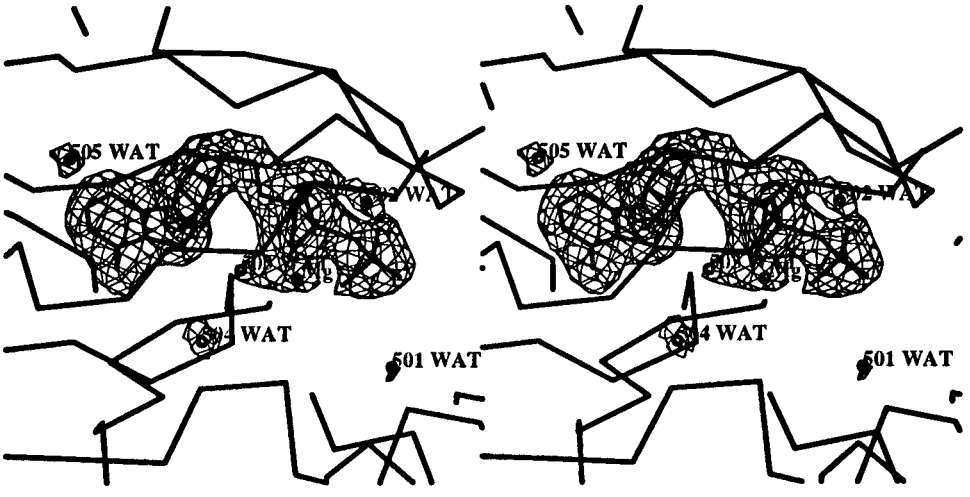

Figure 1. $F_o - F_c$ omit map for ATP, Mg^{2+}, and five water molecules within 4.5 Å of ATP. The map was contoured at 3 σ. The enzyme is schematically drawn as Cα trace and Mg^{2+} and water molecules are displayed as filled black circles.

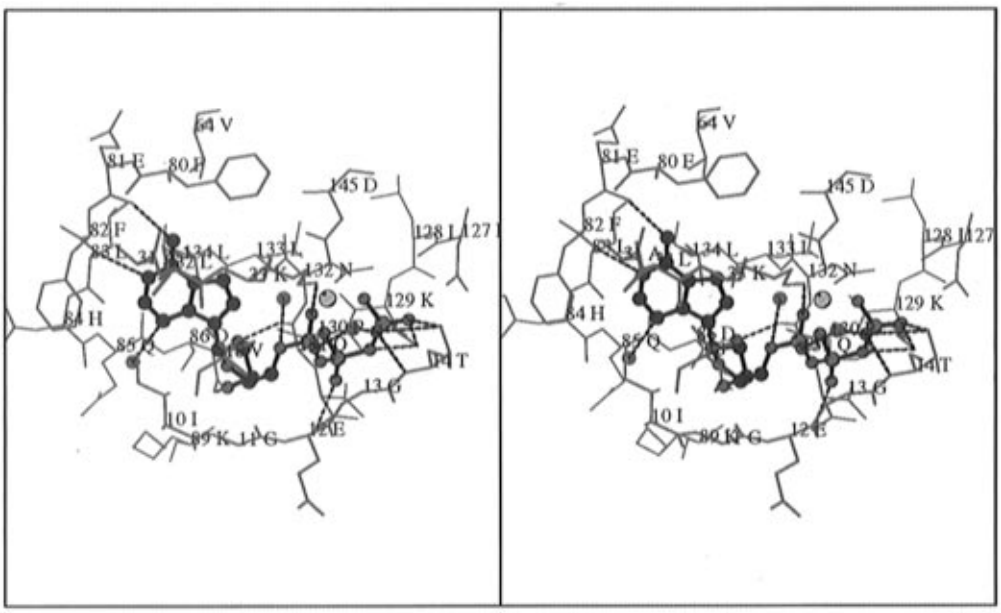

Figure 2. Schematic stereodrawing of the ATP binding pocket in the CDK2−ATP complex. CDK2 residues in contact with ATP are shown in green. ATP and three waters in hydrogen-bonding distance are shown as a ball and stick model with atom-specific coloring: dark gray for carbon, blue for nitrogen, red for oxygen, pink for phosphate, and light gray for Mg^{2+}. Hydrogen bonds are indicated as broken lines.

Table 3. ATP Interactions with CDK2

CDK2 residue	total number of contacts			hydrogen bond partners	
	adenine	ribose	phosphates		
I^{10}	3	2			
G^{13}			6, α + γ	$G^{13}N$	ATP Oα2
T^{14}			8, γ	$T^{14}N$	ATP Oγ2
				$T^{14}O\gamma1$	ATP Oγ2
				$T^{14}\gamma1$	ATP Oγ3
V^{18}	1	4	2, α		
A^{31}	4				
K^{33}			4, α	$K^{33}N\zeta^a$	ATP Oα1
				$K^{33}N\zeta^a$	ATP Oα2
V^{64}	1				
F^{80}	1				
E^{81}	2			$E^{81}O$	ATP N6
F^{82}	4				
L^{83}	3			$L^{83}N$	ATP N1
D^{86}		3		$D^{86}O\delta1$	ATP O3′
K^{129}			7, β + γ	$K^{129}N\zeta^a$	ATP Oγ3
				$K^{129}N\zeta^a$	ATP Oβ3
Q^{131}		3	9, β	$Q^{131}N\epsilon2$	ATP Oβ1
				$Q^{131}O$	ATP O2′
N^{132}			4, β + γ		
L^{134}	4	1			
D^{145}			5, α + γ		
Wat^{502}			4, α + γ	$Wat^{502}O$	ATP Oα2
				$Wat^{502}O$	ATP Oγ2
Wat^{503}	1	2	3, α	$Wat^{503}O$	ATP O5′
Wat^{505}	2			$Wat^{505}O$	ATP N3
total	26	15	52	15	

[a] Salt bridge.

gen and its side-chain carboxylate (Wat^{504}, Figure 5) and through water-mediated hydrogen bonds to backbone carbonyl oxygens of residues His^{125} and Asp^{145} (Wat^{501}, Figure 5). Of the remaining water molecules in the apoenzyme binding pocket, three are very close to the position of N1, N6, and N7 atoms in the adenine ring of the superimposed CDK2−ATP complex and five are located in the binding pocket area for the triphosphate of ATP (Figure 4).

The CDK2 apoenzyme and its ATP complex are structurally very similar with a rms deviation of 0.39 Å for all backbone atoms except residues 37−40. Even residue conformations in the ATP binding pocket are mostly conserved, including residue Gln^{131} with two alternate side-chain conformations (Figure 6). The only significant differences are observed in the side chains of residues Lys^{33}, Lys^{129}, and Asn^{132} (Figure 6). In the CDK2−ATP complex, the Lys^{33} side-chain Nζ atom is positioned close to the ATP α-phosphate and Asp^{145} carboxylate, several angstroms removed from its position in the apoenzyme where it forms hydrogen bonds with Asp^{145} and a water molecule in the binding pocket. Conformational changes for Lys^{129} are smaller. The Nζ atom is within hydrogen-bonding distance to Asp^{127} carboxyl oxygens in the apoenzyme. The observed shift of the Nζ atom in the CDK2−ATP complex moves it closer to the ATP γ-phosphate and away from Asp^{127}. Finally, the conformation of Asn^{132} in the ATP complex positions the side-chain amide close to the Mg^{2+}ATP and provides a coordination partner for the Mg^{2+} ion. In the apoenzyme, the same side chain is pointing away from the binding pocket and forms a hydrogen bond with the backbone nitrogen of Lys^{129}.

ATP Conformation in CDK2 and Other Protein Kinases. The refinement of the CDK2−ATP complex to 1.9 Å provides a very clear picture of the ATP binding mode and ATP interactions with the inactive CDK2. In contrast to the structure of the inactive MAPK where the γ-phosphate of ATP seems disordered,[10] the ATP density is well defined in the CDK2−ATP complex. However, as described earlier,[14] there are conformational differences to the ATP molecule in the active enzyme cAPK.[22] The ribose adopts a C2′-*endo* conformation, compared to the C3′-*endo* puckering in the cAPK structure. More importantly, the position of the β-phosphate is far removed from its position in the ATP−cAPK complex,[22] leading to an almost perpendicular orientation of the $P_\alpha-P_\beta$ and the $P_\beta-P_\gamma$ bonds in the CDK2 and cAPK complex structures. Consequently, the position and coordination of the Mg^{2+} ion is different as well. In the CDK2 complex, we observe only one Mg^{2+} binding site, which is closest to the minor binding site in the cAPK−ATP complex where five ligands for the metal, Pα, Pγ, Asn^{171}, Asp^{184}, and a

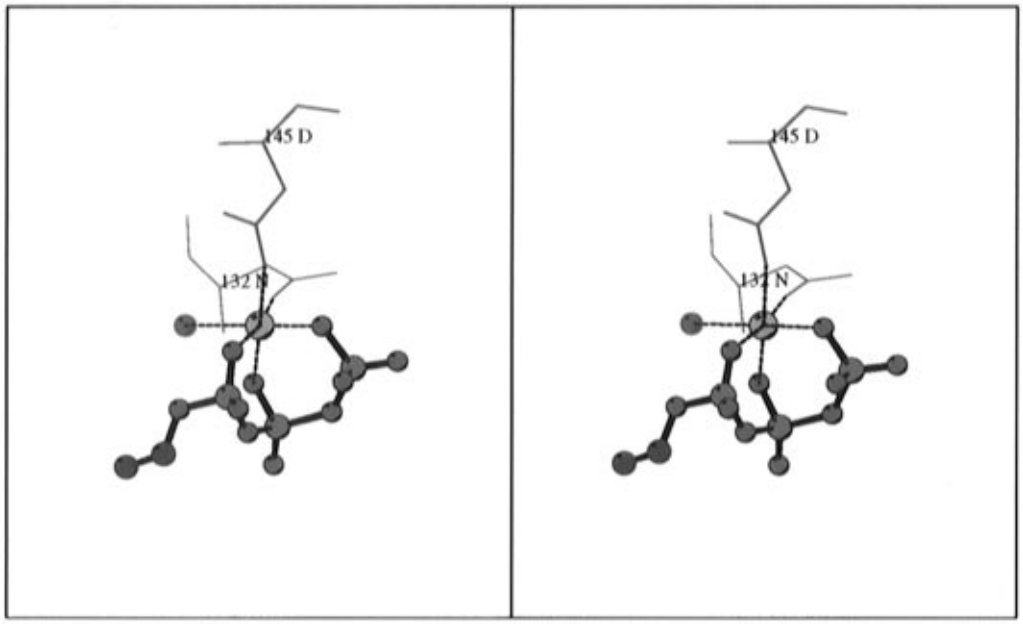

Figure 3. Close-up stereoview of the Mg^{2+} binding site in the CDK2−ATP complex. The orientation and coloring are identical to those in Figure 2. Six oxygen donor ligands are arranged in octahedral geometry around the Mg^{2+} ion.

solvent have been described.[23] The Mg^{2+} ion in the CDK2 complex is coordinated by the same conserved protein residues, Asn^{132}, Asp^{145}, a solvent, and all three phosphates, due to the different positioning of the β-phosphate (Figure 3). Although the electron density in the presumed metal binding site is relatively weak for a Mg^{2+} atom, it was interpretated as Mg^{2+} because of the short coordination bonds (average 2.0 Å) to its ligands, octahedral coordination that is the preferred geometry for alkaline earth metal ions in complexes with oxygen donor groups, and its relation to the minor metal binding site in cAPK.

Implications for CDK2 Inhibitor Design. The natural ligand ATP can be regarded as pseudo lead compound for the structure-based design of small inhibitor molecules of CDK2. The detailed description of the CDK2-ATP complex structure provides a list of potentially important interactions for ligand binding. However, other information such as binding affinities of ligand analogues, conformational flexibility of the ligand, and solvation of residues in the binding pocket of the apoenzyme are needed to identify functionally essential interactions. The list of all CDK2-ATP contacts (Table 3) shows more than half of all contacts, including nine hydrogen bonds, being formed with the triphosphate portion of ATP. However binding studies of cAPK with ATP analogues revealed low sensitivity to modifications in the triphosphate moiety as long as there is an uncharged group in the 5′-position on the ribose moiety.[24] These seemingly contradictory findings might be explained by the high cost of decreased entropy in binding the flexible triphosphate moiety which is counterbalanced by the entropically favorable displacement of water molecules from the binding pocket. Similarly, changes in the net energy of hydrogen bonding should be small since the formation of hydrogen bonds in the CDK2−ATP complex involves the displacement of hydrogen-bonded water molecules. Indeed, the high-resolution structure of the CDK2 apoenzyme shows density for five well-ordered waters in the binding pocket area for the triphosphate (Figure 4).

In contrast to the phosphate contacts, adenine interactions with CDK2 are mostly of hydrophobic nature with residues that are conserved throughout the protein kinase family. Two hydrogen bonds, between $L^{83}N$ and ATP N1 and between $E^{81}O$ and ATP N6 are observed (Table 3), of which the latter was shown to be essential for high-affinity binding of ATP in cAPK.[24] The fact that this hydrogen bond is formed in a hydrophobic environment, which increases the interaction energy between two dipoles, most likely contributes to its importance in overall binding affinity. The binding pocket for the adenine in the apoenzyme shows three well-defined waters whose density overlaps with the adenine ring in the superimposed ATP complex (Figure 4). One of the waters is substituting for the adenine N6 atom forming a hydrogen bond with $E^{81}O$, thereby confirming the importance of a hydrogen-bonding partner for $E^{81}O$. The second is close to N1 and C2 in the adenine ring, forming a hydrogen bond with $Leu^{83}O$ instead of $L^{83}N$, as the N1 atom of adenine does, and the third is close to the N7 atom, forming hydrogen bonds with other water molecules in the binding pocket. The large contribution of the adenine base to binding affinity is probably due to the formation of essential buried hydrogen bonds and numerous van der Waals contacts in combination with the smaller entropic cost of binding the rigid purine ring. The *B*-factor distribution in the ATP molecule, that shows increasing values from the adenine ring to the γ-phosphate, correlates with the atom movements, and probably reflects the strength of CDK2−ATP interactions for the respective atoms.

Binding energies between enzyme and ligand could also be affected by conformational changes in the protein partner. However, analysis of conformational differences between CDK2 apoenzyme and its ATP complex (Figure 6) and other CDK2 inhibitor complexes[19,25] show only adjustments in a few side-chain conformations in response to small molecule ligand binding and very small changes in backbone atoms.

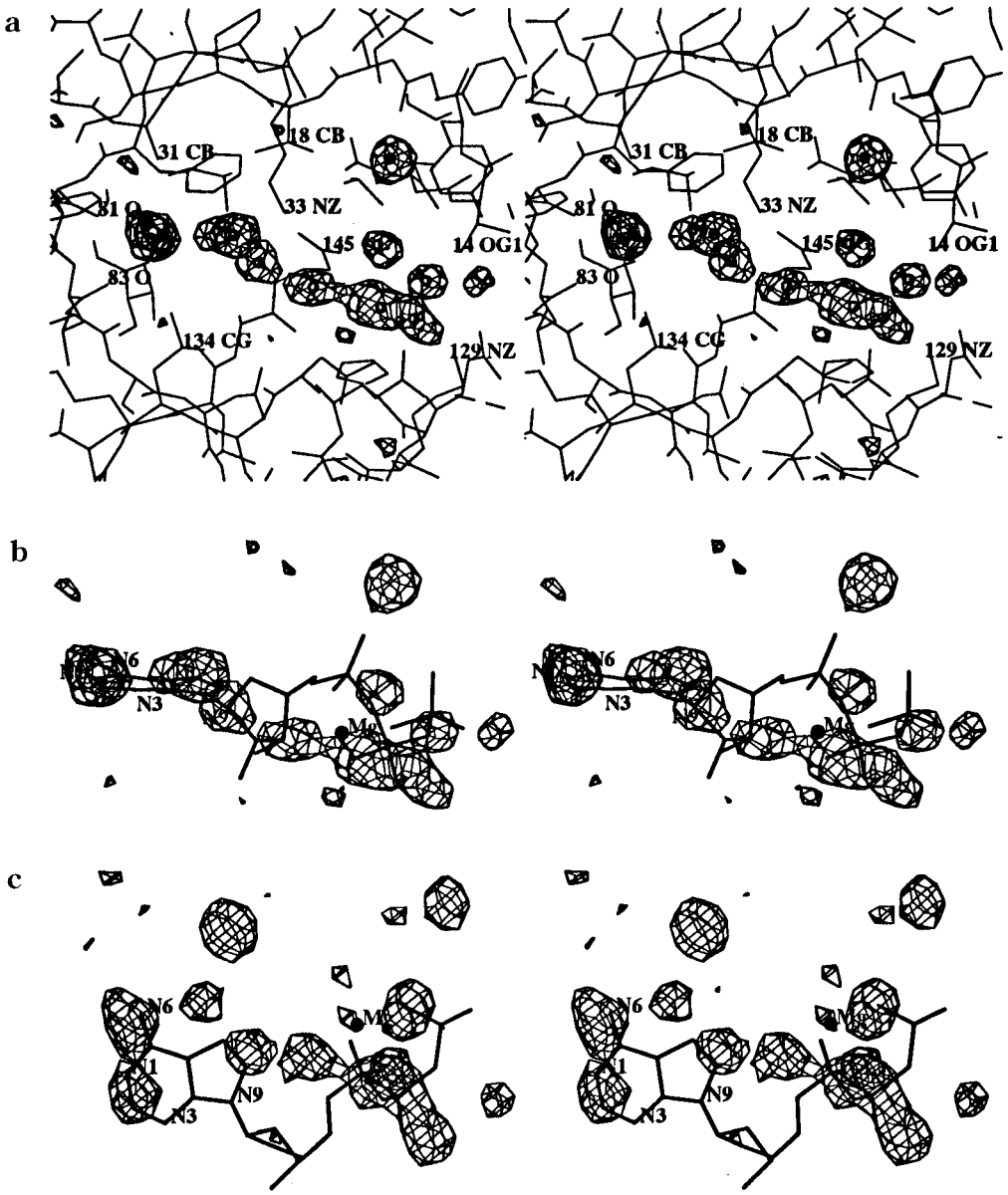

Figure 4. Stereoview of the $F_o - F_c$ omit map for 12 water molecules in the ATP binding pocket of CDK2 apoenzyme. The electron density map was contoured at 3.25 σ. In (a) CDK2 residues that form the binding pocket are shown, and water molecules are drawn as black circles. (b, c) The same omit density for waters in the apoenzyme is shown together with the superimposed ATP molecule imported from the CDK2-ATP complex. Part b is drawn in the same orientation as (a), while (c) is rotated 90° around a horizontal axis.

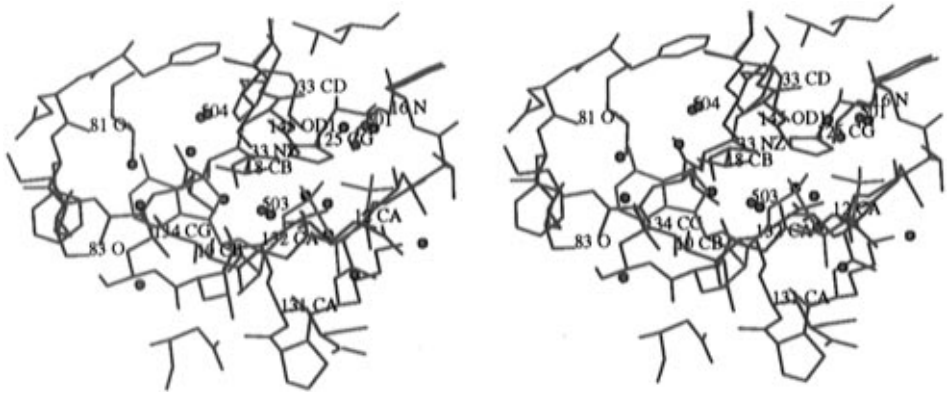

Figure 5. Comparison of the water structure in the ATP binding pocket of CDK2 apoenzyme and its ATP complex. The enzyme and waters in the CDK2−ATP complex are shown in green, ATP in cyan. Waters in the binding pocket of the superimposed apoenzyme are shown in red, as well as the side chain of Lys[33] which adopts a very different conformation in the CDK2−ATP complex. Some enzyme residues, as well as those water molecules, that are found in similar locations in the apoenzyme and CDK2−ATP complex are labeled.

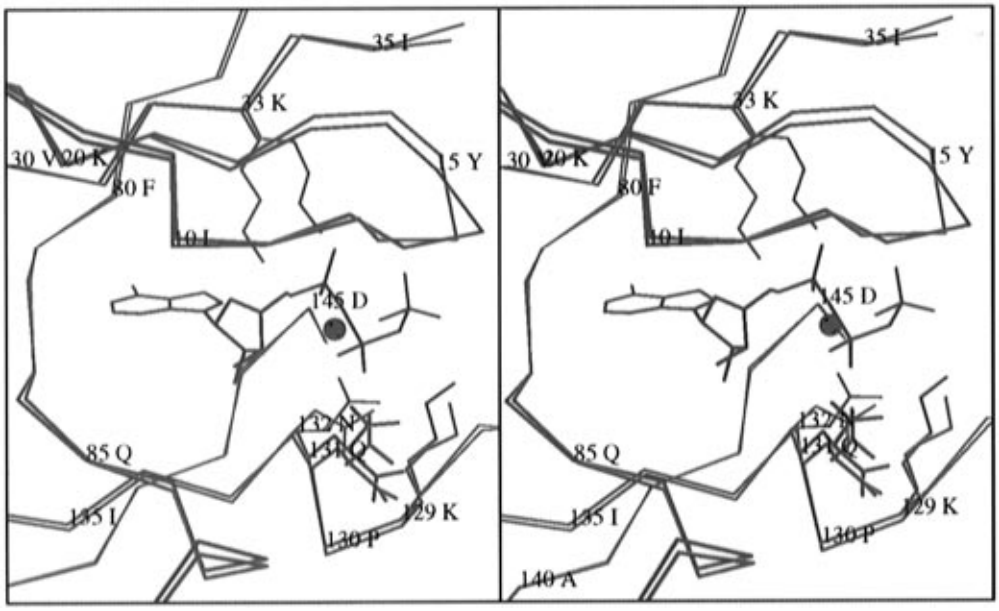

Figure 6. Schematic stereodrawing of the ATP binding pocket in the CDK2 apoenzyme and its ATP complex after superposition. The CDK2−ATP complex is drawn in green, the apoenzyme in red. Side chains whose conformation differ significantly between the two structures are shown, as well as the side chain of Gln^{131} that adopts alternate side-chain conformations in both structures. The Mg^{2+} ion is shown as a filled green circle.

Conclusion

Analysis of the high-resolution structures of CDK2 apoenzyme and its ATP complex provides important information for the structure-based design of new drugs and the improvement of already identified lead compounds.

(1) The water structure of the binding pocket suggests binding partners for potential ligands. However, the energetics of displacing bound waters with ligand atoms has to be considered.

(2) The number of observed protein−ligand hydrogen bonds does not always correlate with the importance of the respective ligand moiety for binding affinity. If the ligand displaces hydrogen-bonded water molecules, the net changes in hydrogen-bonding energy might be small. In addition, the entropically favorable displacement of waters might be balanced by the unfavorable immobilization of ligand atoms.

(3) Ligand-induced conformational changes in the protein are difficult to predict and need to be determined experimentally. In case of CDK2, they are small and probably not important.

(4) A relatively small number of directional hydrogen bonds compared to nondirectional hydrophobic interactions might allow a larger variety of chemical scaffolds for inhibitor design and more flexibility in the orientation of inhibitor binding. For example, the adenine binding pocket of CDK2 can accommodate adenine-based inhibitors in three different orientations[19] as well as a flavopiridol-based inhibitor.[25] However, more examples will show if this is true in general.

Experimental Methods

Human CDK2 was expressed in SF9 cells with a recombinant baculovirus vector, purified, and crystallized as described previously.[26] Diamond and wedge-shaped crystals appeared after 2−4 days and continued growing after gradual increases of the buffer concentration in the reservoir. The Mg^{2+}ATP−CDK2 complex was obtained by cocrystallization and by soaking apoenzyme crystals in 50 mM HEPES solution, pH 7.4, containing 2.5 mM $MgCl_2$ and 1.25 mM ATP for 48 h. The size of the apoenzyme crystal was 0.35 × 0.25 × 0.25 mm and that of the Mg^{2+}ATP−CDK2 complex was 0.30 × 0.20 × 0.20 mm.

Diffraction data were collected at room temperature from a single crystal with a Rigaku RAXIS-II imaging plate area detector using 1.6° or 1.7° oscillation angles for the apoenzyme and complex crystal, respectively. Data were processed with the Raxis data processing software (Table 1). Refinement of the apoenzyme structure to 1.8 Å resolution was performed using X-PLOR[27] with the 2.4 Å resolution apoenzyme structure as the starting model. Rounds of simulated annealing using the slow-cooling protocol, followed by individually restrained *B*-factor refinement, were alternated with rebuilding of parts of the enzyme and all water molecules into $2F_o - F_c$ or $F_o - F_c$ omit maps, using the program O.[28] The model was rebuilt into SIGMAA-weighted simulated annealing omit maps[29] where parts of the enzyme or solvent molecules were omitted for structure factor calculation. Only those regions of the enzyme with high *B* values in the 2.4 Å structure were rebuilt. Finally, additional waters within hydrogen-bonding distances to acceptor or donor protein atoms were built into $F_o - F_c > 3\sigma$ densities, and alternate side-chain positions for residues Gln^{131} and Ser^{264} were included. The final structure has a R_{free} of 25.45% and R_{cryst} of 18.12% for 8−1.8 Å data with $F/\sigma F > 2.0$ and good stereochemistry (Table 2). Residues 37−40 were excluded from the final model because of extremely weak and disconnected electron density.

Refinement of the Mg^{2+}ATP−CDK2 complex proceeded similarly. However, the whole enzyme, ATP, and solvent molecules were checked and if neccessary rebuild into 10% omit maps. The final complex structure has a R_{free} of 27.2% and R_{cryst} of 18.47% for 8−1.9 Å data with $F/\sigma F > 2.0$ and good stereochemistry (Table 2). As in the apoenzyme, residues 37−40 were omitted in the final model because of missing electron density.

Root mean square differences on backbone atoms were calculated with the Protein Analysis Package (PAP).[30] Proteins were superimposed on Cα atoms using the program OVRLAP[31] with the simple progression rule. Hydrogen bonds and van der Waals contacts were assigned with the program CONTACSYM.[32] The cutoff for hydrogen bonds and salt bridges was 3.4 Å and up to 4.11 Å for van der Waals contacts, depending on the atom type and using standard van der Waals radii.

References

(1) Hanks, S. K.; Quinn, A. M.; Hunter, T. The Protein Kinase Family: Conserved Features and Deduced Phylogeny of the Catalytic Domains. *Science* **1988**, *241*, 42−52.

(2) Blumer, K. J.; Johnson, G. L. Diversity in Function and Regulation of MAP Kinase Pathways. *Trends Biochem. Sci.* **1994**, *19*, 236−240.

(3) Davis, R. J. MAPKs: New JNK Expands the Group. *Trends Biochem. Sci.* **1994**, *19*, 470−473.

(4) Marshall, C. J. Specificity of Receptor Tyrosine Kinase Signaling: Transient versus Sustained Extracellular Signal-Regulated Kinase Activation. *Cell* **1995**, *80*, 179−185.

(5) Schultz, J.; Ferguson, B.; Sprague, G. F., Jr. Signal Transduction and Growth Control in Yeast. *Curr. Opin. Genet. Dev.* **1995**, *5*, 31−37.

(6) Norbury, C.; Nurse, P. Animal Cell Cycles and their Control. *Annu. Rev. Biochem.* **1992**, *61*, 441−470.

(7) Nigg, E. A. Targets of Cyclin-Dependent Protein Kinases. *Curr. Opin. Cell Biol.* **1993**, *5*, 187−193.

(8) Morgan, D. O. Principles of CDK Regulation. *Nature* **1995**, *374*, 131−134.

(9) Knighton, D. R.; Zheng, J.; Ten Eyck, L. F.; Ashford, V. A.; Xuong, N.-H.; Taylor, S. S.; Sowadski, J. M. Crystal Structure of the Catalytic Subunit of Cyclic Adenosine Monophosphate-Dependent Protein Kinase. *Science* **1991**, *253*, 407−414.

(10) Zhang, F.; Strand, A.; Robbins, D.; Cobb, M. H.; Goldsmith, E. J. Atomic Structure of the MAP Kinase ERK2 at 2.3 Å Resolution. *Nature* **1994**, *367*, 704−711.

(11) Hu, S.-H.; Parker, M. W.; Lei, J. Y.; Wilce, M. C. J.; Benian, G. M.; Kemp, B. E. Insights into Autoregulation from the Crystal Structure of Twitchin Kinase. *Nature* **1994**, *369*, 581−584.

(12) Xu, R.-M.; Carmel, G.; Sweet, R. M.; Kuret, J.; Cheng, X. Crystal Structure of Casein Kinase-1, a Phosphate-Directed Protein Kinase. *EMBO J.* **1995**, *14*, 1015−1023.

(13) Owen, D. J.; Noble, M. E.; Garman, E. F.; Papageorgiou, A. C.; Johnson, L. N. Two Structures of the Catalytic Domain of Phosphorylase Kinase: An Active Protein Kinase Complexed with Substrate Analogue and Product. *Structure* **1995**, *3*, 467−482.

(14) DeBondt, H. L.; Rosenblatt, J.; Jancarik, J.; Jones, H. D.; Morgan, D. O.; Kim, S.-H. Crystal Structure of Cyclin-Dependent Kinase 2. *Nature* **1993**, *363*, 595−602.

(15) Taylor, S. S.; Radzio-Andzelm, E. Three Protein Kinase Structures Define a Common Motif. *Structure* **1994**, *2*, 345−355.

(16) Kitagawa, M.; Okabe, T.; Ogino, H.; Matsumoto, H.; Suzuki-Takahashi, I.; Kokubo, T.; Higashi, H.; Saitoh, S.; Taya, Y.; Yasuda, H.; Ohba, Y.; Nishimura, S.; Tanaka, N.; Okuyama, A. Butyrolactone I, a Selective Inhibitor of CDK2 and CDC2 Kinase. *Oncogene* **1993**, *8*, 2425−2432.

(17) Losiewicz, M. D.; Carlson, B. A.; Kaur, G.; Sausville, E. A.; Worland, P. J. Potent Inhibition of CDC2 Kinase Activity by the Flavonoid L86-8275. *Biochem. Biophys. Res. Commun.* **1994**, *201*, 589−595.

(18) Vesely, J.; Havlicek, L.; Strnad, M.; Blow, J. J.; Donella-Deana, A.; Pinna, L.; Letham, D. S.; Kato, J.-y.; Detivaud, L.; Leclerc, S.; Meijer, L. Inhibition of Cyclin-Dependent Kinases by Purine Analogues. *Eur. J. Biochem.* **1994**, *224*, 771−786.

(19) Schulze-Gahmen, U.; Brandsen, J.; Jones, H. D.; Morgan, D. O.; Meijer, L.; Vesely, J.; Kim, S.-H. Multiple Modes of Ligand Recognition: Crystal Structures of Cyclin-Dependent Protein Kinase 2 in Complex with ATP and Two Inhibitors, Olomoucine and Isopentenyladenine. *Proteins* **1995**, *22*, 378−391.

(20) Luzzati, V. Treatment of Statistical Errors in the Determination of Crystal Structures. *Acta Crystallogr.* **1952**, *5*, 802−810.

(21) Ramachandran, G. N.; Sasisekharan, V. Conformation of Polypeptides and Proteins. *Adv. Protein Chem.* **1968**, *23*, 283−437.

(22) Zheng, J.; Knighton, D. R.; Ten Eyck, L. F.; Karlsson, R.; Xuong, N.-H.; Taylor, S. S.; Sowadski, J. M. Crystal Structure of the Catalytic Subunit of cAMP-Dependent Protein Kinase Complexed with MgATP and Peptide Inhibitor. *Biochemistry* **1993**, *32*, 2154−2161.

(23) Zheng, J.; Trafny, E. A.; Knighton, D. R.; Xuong, N.-H.; Taylor, S. S.; Ten Eyck, L. F.; Sowadski, J. M. 2.2 Å Refined Crystal Structure of the Catalytic Subunit of cAMP-Dependent Protein Kinase Complexed with MnATP and a Peptide Inhibitor. *Acta Crystallogr.* **1993**, *D49*, 362−365.

(24) Bhatnagar, D.; Roskoski, R., Jr.; Rosendahl, M. S.; Leonard, N. J. Adenosine Cyclic 3′,5′-Monophosphate Dependent Protein Kinase: A New Fluorescence Displacement Titration Technique for Characterizing the Nucleotide Binding Site on the Catalytic Subunit. *Biochemistry* **1983**, *22*, 6310−6317.

(25) Azevedo, W. F., Jr.; Mueller-Dieckmann, H.-J.; Schulze-Gahmen, U.; Worland, P. J.; Kim, S.-H. Structural Basis for Specificity and Potency of a Flavonoid Inhibitor of Human CDK2, a Cell Cycle Kinase. *Proc. Natl. Acad. Sci. U.S.A.* **1996**, *93*, 2735−2740.

(26) Rosenblatt, J.; DeBondt, H.; Jancarik, J.; Morgan, D. O.; Kim, S.-H. Purification and Crystallization of Human Cyclin-Dependent Kinase 2. *J. Mol. Biol.* **1993**, *230*, 1317−1319.

(27) Brünger, A. T. *X-PLOR, Version 3.1: A System for Crystallography and NMR*; Yale University Press: New Haven, CT, 1992.

(28) Jones, T. A.; Zou, J.-Y.; Cowan, S. W.; Kjeldgaard, M. Improved Methods for Binding Protein Models in Electron Density Maps and the Location of Errors in these Models. *Acta Crystallogr.* **1991**, *A47*, 110−119.

(29) Collaborative Computational Project, Number 4 The CCP4 Suite: Programs for Protein Crystallography. *Acta Crystallogr.* **1994**, *D50*, 760−763.

(30) Callahan, T.; Gleason, W. B.; Lybrand, T. P. "PAP": A Protein Analysis Package. *J. Appl. Crystallogr.* **1990**, *23*, 434−436.

(31) Rossmann, M. G.; Argos, P. A Comparison of the Heme Binding Pocket in Globins and Cytochrome b_5. *J. Biol. Chem.* **1975**, *250*, 7525−7532.

(32) Sheriff, S.; Hendrickson, W. A.; Smith, J. L. Structure of Myohemerythin in the Azidomet State at 1.7/1.3 Å Resolution. *J. Mol. Biol.* **1987**, *197*, 273−296.

JM960402A